Heat transfer framework for selecting the structure of open volumetric air receivers

Cristóbal Sarmiento[1], José Cardemil[1], Williams Calderón[1] and Benjamín Herrmann[1]
[1] Mechanical Engineering Department / Universidad de Chile, Beauchef 851, Santiago (Chile).

Abstract

During the last 10 years, the interest of several authors in the use of compressible gases (as CO_2 and Air) as working fluid in concentrated solar power systems (CSP) has increased significantly. These fluids allow to increase the upper limit of the operating temperatures and achieve higher conversion efficiencies. Nevertheless, achieving temperatures higher than 700°C requires the use of volumetric absorbers, which design presents two scientific challenges. The first related to the computational modeling of the transport phenomena inside the porous media, coupling the viscous effects, compressibility, the convective heat transfer and the extinction-propagation of the concentered radiation in the solid media. And the second, related to the design process regarding the configuration, distribution and material selection of the solid media, aiming to deal with the challenging operating conditions. In that context, the present study presents a performance analysis of an open volumetric absorber using atmospheric Air as working fluid, comparing honeycomb mini-channel (HC) and ceramic foam (CF) as exchange solid media. The results show that the ceramic foam is the better option for the total range of porosity analyzed, accordingly to the novel figure of merit proposed in this document. The proposed benefit factor considers the benefit related to the capacity of heat exchange and the power losses by pressure drop inherent of each design in study.

Keywords: Honeycomb mini-channel, Ceramic foam, Porous media, and Volumetric absorber.

1. Introduction

After the initial development in the ’80s, the CSP industry has experienced considerable growth since 2007 (Avila-Marin, 2011; Kribus, Ries, & Spirkl, 1996). In this period, new technologies have reached commercial maturity and new concepts have emerged. Among the CSP technologies, central receiver systems (CRS) have received larger attention during the last years, since the higher operating temperatures allow reaching higher thermal-to-electricity conversion efficiencies. In this context, two main operating schemes have emerged for this technology: Direct Steam Generation and Molten Nitrate Salts receivers, which are denominated as the first and second generation, respectively. Aiming to further improve the conversion efficiencies, several authors proposed the use of compressible gases (CO_2 and Air) as working fluid, due to its thermal stability up to 1200°C. The use of such working fluids requires the implementation of volumetric absorbers. Among the compressible gases, Air offers additional advantages by the lower operating pressure and cost, when using atmospheric air in open receiver systems. A volumetric receiver for atmospheric air implies the incorporation of solid porous media as heat exchange medium, between the solar radiation and the working fluid.

Despites several configurations for volumetric receivers have been proposed in the literature (Avila-Marin, 2011), the present analysis is focused to compare two of the most studied configurations, honeycomb mini-channel (HC) and ceramic foam (CF). The HC structure presents simplicity for the manufacturing process and offers low-pressure drop. On the other hand, the CF proposal presents outstanding heat exchange capabilities, due to its larger exchange area, but increasing the pressure drop (Chen, Xia, Yan, & Sun, 2017; Kribus et al., 2014; Wu, Caliot, Flamant, & Wang, 2011b). Therefore, this relation, between the benefits of increasing the exchange area and the disadvantages of the pressure drop involved, encourages the analysis presented herein. Thus, aiming to establish a comparison framework between both technologic options, the methodology proposes a figure of merit able to assess and compare the performance of CF and HC, including the heat exchange benefits and pressure drop involved at the same time. The computational modelling of both technologies was performed through an one-dimensional (1D) model at the same operating conditions for each technology.

2. Methodology

The 1D model for both structures was developed in MATLAB using the Runge Kutta numerical method. The system of equations for each kind of absorber considers a) Conservation of mass of the fluid domain, b)

doi:10.18086/swc.2019.18.11 Available at http://proceedings.ises.org

conservation momentum of the flow, c) conservation of energy in the solid and the fluid domain. In addition to that, each energy conservation in the solid medium considers a font term for accounting the propagation of the radiation in the solid (considering extinction and emission effects). Likewise, some assumptions were considered in order to simplify the analysis, considering that the model solves both systems (HC and CF) at the same time. Thus, the assumptions are as follow:

- Conduction effects through in the fluid are neglected in both models.
- Radiative absorption at the fluid phase is neglected in both systems.
- Both processes are in steady-state.
- The air is considered as an ideal gas.
- Isotropic distribution of CF porosity.
- Momentum diffusion by viscous effects inside the fluid is neglected in both systems.
- Isolated system on the parallel walls to the flow direction.

From the afore assumptions, the following equations express the mass, momentum and energy transport for a honeycomb mini-channel and ceramic foam volumetric absorber, considering the same geometrical parameters and boundary conditions (see Fig. 1), as follows:

- The comparison velocity is u_c = 1 m s^{-1}, which is considered as apparent u_D velocity for the ceramic foam and, on the other hand, the comparison velocity is divided by the porosity and used as the pore real velocity (pore velocity in porous media analysis).
- The pore diameter in the ceramic is equal to the mini-channel in the honeycomb.
- The axial area of the receiver is square with high length $l = 0.05$ m.
- The incident radiation is fixed at $I_0 = 600$kW/m^2.

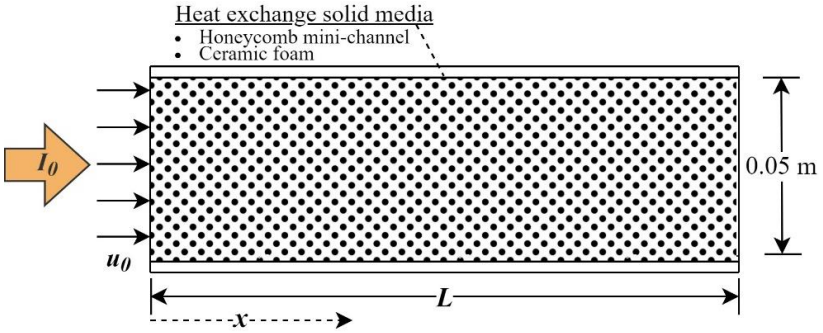

Figure 1. **Diagram of the volumetric absorber**

Honeycomb's mathematical model

Continuity and momentum transport equations

$$\nabla \cdot (\rho_f u) = 0 \quad \text{(eq. 1)}$$

$$\nabla \cdot (\rho_f uu) = -\nabla(P) - F_{HC} \quad \text{(eq. 2)}$$

where u is the mini-channel mean velocity, ρ_f the fluid density, P is the fluid's thermodynamic pressure and F_{HC} the pressure drop term. The pressure drop term was determined as follow:

$$F_{HC} = f\frac{\rho_f}{2l}u^2 \quad \text{(eq. 3)}$$

where l is the mini-channel axial length, f the friction factor concerning to a square channel (Bejan, 2013).

The energy transport in both systems (HC and CF) was solved considering the local non-thermal equilibrium approach (Kaviany, 1999), which considers two different equations for the solid and fluid phases.

Fluid energy transport equation

$$\nabla \cdot (\rho_f c_{p,f} u T_f) = h(T_s - T_f) \quad \text{(eq. 4)}$$

where $c_{p,f}$ is the thermal capacity, T_f the temperature of fluid, T_s the temperature of the solid wall and h the convective heat transfer coefficient (Bejan, 2013).

Solid energy transport equation

$$\nabla \cdot (\lambda_s \nabla T_s) = h\left(T_s - T_f\right) + \mathrm{S}_{r,HC} \quad \text{(eq. 5)}$$

where λ_s is the thermal conductivity of the solid phase and $\mathrm{S}_{r,HC}$ the radiative heat source in the solid phase. The source term related to the propagation of the radiation in the HC structure considers the equation proposed by Worth et al. (Worth, Spence, Crumpton, & Kolaczkowski, 1996), which considers the emission and absorption effects of the radiation entering the square mini-channel.

Ceramic Foam's mathematical model

Continuity and momentum transport equations

$$\nabla \cdot (\rho_f u_D) = 0 \quad \text{(eq. 6)}$$

$$\nabla \cdot \left(\frac{\rho_f u_D u_D}{\phi}\right) = -\nabla(\phi \langle P \rangle^i) - \phi(F_{CF}) \quad \text{(eq. 7)}$$

where ϕ is the porosity, the symbol $\langle \quad \rangle^i$ represent the volume average (Hsu & Cheng, 1990; Kaviany, 1999; Lage, De Lemos, & Nield, 2012), u_D the apparent velocity, defined as $u_D = \phi \langle u \rangle^i$, where $\langle u \rangle^i$ is the pore scale average velocity. Also, $\langle P \rangle^i$ is the volume average fluid's thermodynamic pressure and F_{CF} represent the drag force done by the solid matrix in opposition to the mean flow, in other terms, called the hydrodynamic resistance from Darcy-Forchheimer's law (Lage et al., 2012), as follows:

$$F_{CF} = \frac{\mu_f}{k_1} u_D + \frac{\rho_f}{k_2} |u_D| u_D \quad \text{(eq. 8)}$$

where μ_f is the fluid dynamic viscosity, both k_1 and k_2, are correlation constants determined by Wu's correlation (Wu et al., 2010). Thus, the right terms in eq. 8 represent the normal and tangential forces done by the solid matrix over the fluid´s mean flow, respectively.

Fluid energy transport equation

$$\nabla \cdot \left(\rho_f c_{p,f} u_D \langle T_f \rangle^i\right) = h_v\left(\langle T_s \rangle^i - \langle T_f \rangle^i\right) \quad \text{(eq. 9)}$$

where $\langle T_f \rangle^i$ is the volume average temperature of the fluid, $\langle T_s \rangle^i$ the volume average temperature of the solid wall and h_v the local volumetric heat transfer coefficient (Hsu & Cheng, 1990; Lage et al., 2012). This last coefficient was determined by the correlation proposed by Wu et al. (Wu et al., 2011b).

Solid energy transport equation

$$\nabla \cdot \left(\lambda_s \nabla(\phi \langle T_s \rangle^i)\right) = h_v\left(\langle T_s \rangle^i - \langle T_f \rangle^i\right) + \mathrm{S}_{r,CF} \quad \text{(eq. 10)}$$

In addition, to determine the radiative source $\mathrm{S}_{r,CF}$, is necessary to solve the radiative transfer equation (RTE) in the solid. Thus, the P1 (Andrienko & Surzhikov, 2012; Chen et al., 2017; Modest, 2013; Wu, Caliot, Flamant, & Wang, 2011a) approximation model was implemented to solve the RTE, as follows.

Radiative heat transfer equation

$$\nabla \cdot \left(\frac{1}{3(k + \sigma_s)} \nabla G_s\right) = k\left(4\sigma \langle T_s \rangle^{i\,4} + G_s\right) + \sigma_s G_c \quad \text{(eq. 11)}$$

where σ is the Stefan–Boltzmann constant, k the absorption coefficient, σ_s the scattering coefficient, β the extinction coefficient, G is the total irradiation, G_s the diffuse integrated intensity and G_c the collimated irradiation in the flow direction (x). Also, considering as following expressions the radiative heat source in solid's phase is determined as follow,

$$G_c = I_0 e^{-\beta x} \quad \text{(eq. 12)}$$

$$G = G_c + G_s \quad \text{(eq. 13)}$$

$$\beta = k + \sigma_s \quad \text{(eq. 14)}$$

$$S_{r,CF} = -k\left(G - 4\sigma\langle T_s\rangle^{i\,4}\right) \quad \text{(eq. 15)}$$

Aforementioned optical properties were computed considering the optical approximations for porous media proposed by Vafai (Vafai, 2015).

Aiming to analyze and compare the performance of the honeycomb and ceramic foam volumetric receivers, it is proposed a modification of the goodness factor proposed initially by Bergles (Bergles, Junkhan, & Bunn, 1976; Shah, 2003). In essence, this figure of merit compares the heat transfer capacity of different heat exchange devices, including a penalization which accounts for the pressure drop associated in each case. Nevertheless, Bergles' goodness factor is commonly applied considering average properties (as temperature and fluid velocity) in each side of heat exchange, or in other cases, the logarithmic mean temperature difference between hot and cold sides of the analyzed exchange device. For this analysis, the volumetric goodness factor is integrated through the receiver to compare the real total amount of exchanged energy per unit of time with the total power lost by the hydrodynamic effects. The volumetric goodness factor is defined as follows:

$$GF_{HC} = \int_0^L \frac{h\left(T_s - T_f\right)}{\rho_f u(F_{HC})}\,dx \quad \text{(eq. 16)}$$

$$GF_{CF} = \int_0^L \frac{h_v\left(\langle T_s\rangle^i - \langle T_f\rangle^i\right)}{\rho_f \langle u\rangle^i (F_{CF})}\,dx \quad \text{(eq. 17)}$$

where L is the total length of the receiver in flow's direction, GF the volumetric total goodness factor, HC and CF subscripts represent both technologic proposals honeycomb and ceramic foam, respectively.

Finally, both benefit figures of merit are confronted in the comparison factor, which allows determining which technology is better considering different design configurations.

$$\Psi = \frac{GF_{CF}}{GF_{HC}} \quad \text{(eq. 18)}$$

Boundary conditions

Both systems, CF and HC, were solved using Runge-Kutta's method, considering 5 and 7 boundary conditions respectively. Both analyses consider 5 boundary equations at the inlet side ($x = 0$) to solve the mass, momentum and energy equations, plus one condition shot at the inlet and varied until it reaches an additional condition at the outlet side ($x = L$), as follows:

Continuity and Momentum transport equation:

- $u|_{x=0} = 1$ m s^{-1}
- $P|_{x=0} = 101.314$ kPa

(eq. 19)

Energy transport equation for fluid-phase:

- $T_f\big|_{x=0} = 298.15$ K

(eq. 20)

Energy transport equation for solid-phase:

- $T_s|_{x=0} = T_{s,shoot}$
- $q_s|_{x=0} = -k\left(\sigma\left({T_{s,shoot}}^4 - {T_\infty}^4\right) + I_0\right)$
- $q_s|_{x=L} = 0$ kW m^{-2}

(eq. 21)

In addition, to solve the RTE equation on the ceramic foam receiver were considered Marshak's boundary conditions (Krittacom & Kamiuto, 2009), as follows:

- $G|_{x=0} = I_0$
- $\frac{1}{3(k+\sigma_s)}\nabla G\Big|_{x=0} = 2\sigma {T_\infty}^4 - \frac{G|_{x=0}}{2}$

(eq. 22)

3. Results

One of the main challenges in the literature about volumetric receivers is the absence of a comparison figure of merit, able to include the principal effects of the design over the benefit in one control value. For that reason, the present results show the temperature distribution of two technological proposals, intending to analyze two very different mediums faced in a reasonable way.

Fig. 2 and 4 show the temperature distribution considering different material porosities, for a ceramic foam and honeycomb receiver, respectively. In both, honeycomb and ceramic foam, the inlet velocity is defined as a boundary condition at 1 m/s (for ceramic foam corresponds to the real velocity). For each medium the porosity has a significative influence in solid's inlet temperature, ranging its value between ~800 K to ~110 K for CF and ~700 K to ~900 K for HC, considering porosities from 0.5 to 0.9.

Regarding the ceramic foam (Fig. 2), an increase in the porosity causes a decline in the solid's axial area at the inlet face, decreasing the outlet temperature and the total length of the receiver. That length represents the necessary distance to reach thermal equilibrium between the solid and fluid phases temperatures, which ranges from 0.01 to 0.025 m when the porosity takes values from 0.5 to 0.9, respectively. The porosity has a direct impact on the penetration of the radiation through the solid, which is strongly related to the solid temperature and receiver's equilibrium length at the same time. Thus, the solid temperature at the inlet shows a decrease when the porosity varies from 0.5 to 0.7 reaching its minimum value at a porosity of 0.7. Then, for porosities over 0.7 the solid's temperature increase. This phenomenon is due to two simultaneous effects, first, a lower porosity implies an increment in the solid axial area of the receiver, increasing the amount of radiative energy captured by the solid near the inlet side, then the temperature of solid rises. Nevertheless, for porosities over 0.7, the previous effect loses significance against that the fact that the increasing the porosity dismisses the mass of solid, and so the temperature in the solid face increases again. On the other hand, lower porosity values imply an increase in the extinction coefficient, which in consequence, reduces the penetration length of the radiation through the solid matrix (see Fig. 3). Thus, a variation in the porosity has an important influence in the radiative source distribution inside the solid, which reaches higher values near the inlet side with a high rate of decrease in the flow direction for lower porosities, and on the other hand, normalizes its distribution in the flow direction for higher porosities.

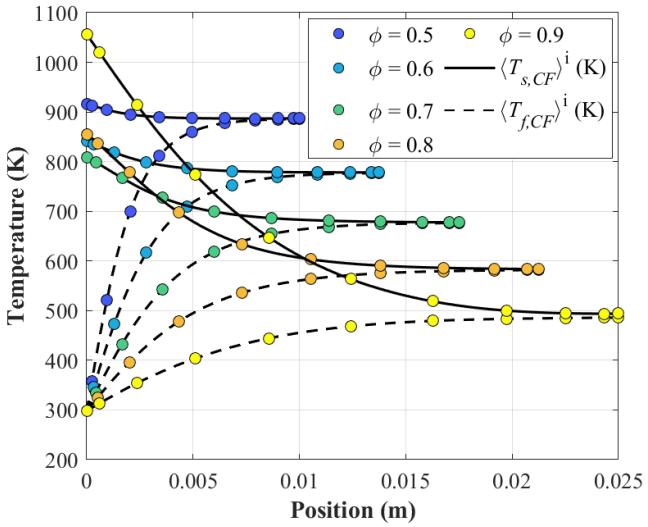

Figure 2. **Temperature distribution for the solid and fluid phase in the flow direction, for a Ceramic Foam porous media in the receiver. Considering a fix mass flow.**

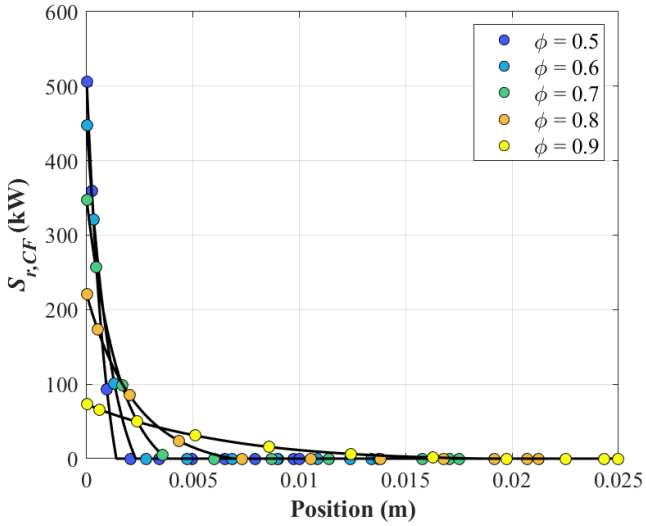

Figure 3. **Radiative source distribution in the flow direction for the ceramic foam. Considering a fix mass flow.**

The honeycomb receiver (Fig. 4) shows an opposite effect with the change of porosity in comparison to the aforementioned results regarding ceramic foam receiver. This is due to the configuration of the mini-channels of the honeycomb. Mini-channel configuration allows that the radiation, normal to the receiver and proportional to ϕ (fluid portion), to pass across the medium without interacting with solid's walls inside the channel, reducing considerably the amount of radiative energy which reaches the inner wall of the solid. Also, the necessary length to achieve the thermal equilibrium presents ranges from 0.015 to 0.06 m, using more material than the ceramic foam to reach the thermal equilibrium. This difference is due to the way that the different solid media exchange heat with the working fluid. The honeycomb mini-channel offers less heat exchange area per unit of length between solid and fluid phases than the ceramic foam. Nevertheless, this advantage for the ceramic foam implies that the fluid is in constant contact against the inner pore walls (Wu et al., 2010), increasing the irreversibilities related to the drag forces associated to the presence of the solid matrix, commonly illustrated as pressure drop terms of Darcy-Forchheimer's law (Kaviany, 1999).

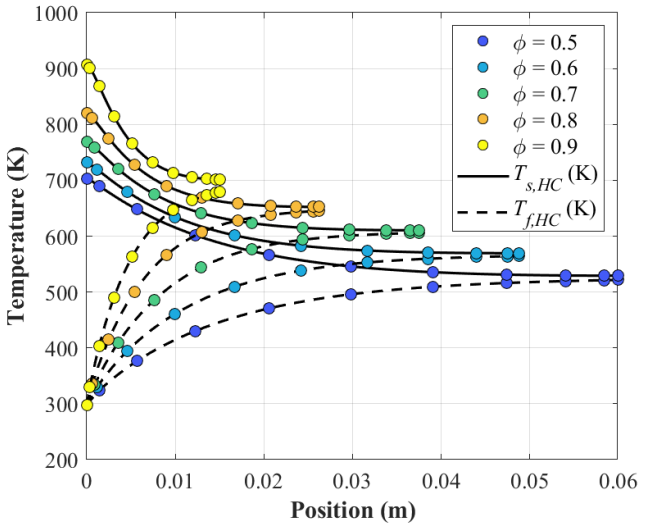

Figure 4. **Temperature distribution for the solid and fluid phase in the flow direction, for a honeycomb porous media in the receiver. Considering a fix mass flow.**

Figure 5 shows the outlet temperature of the fluid in both proposals, and the result of the comparison factor, which faces the goodness factor of both technologies. It is interesting to note how the comparison factor shows one order magnitude in all the complete range of porosity, indicating that the ceramic foam has better performance in all the studied design porosities. This result is unexpected considering that the ceramic foam has a bigger hydrodynamic resistance than the honeycomb, due to the inherent tortuosity of flow's path lines inside the ceramic foam solid matrix (Kaviany, 1999). Nevertheless, the definition of the volumetric goodness factor considers the complete effect of power losses by pressure drop along with the receiver, which is strongly

associated with the receiver's length, and for this analysis, the total length of the HC is more than double of CF length. Thus, despite the ceramic foam presents a higher hydrodynamic resistance, its impact on the volumetric goodness factor is not significant enough than its benefit related to the heat transferred to the fluid.

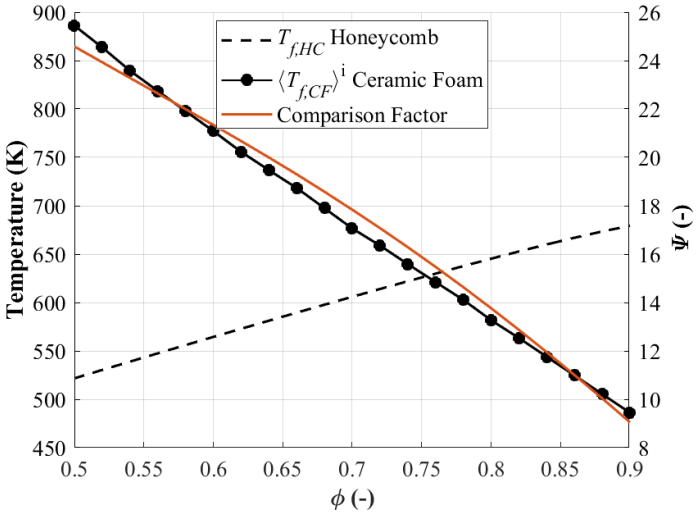

Figure 5. Comparison factor and fluid outlet temperature, for different porosities, considering a fix inlet fluid velocity of 1 m/s.

Figure 6. Shows the volumetric goodness factor of both technical proposals considering porosities from 0.5 to 0.9. Similarly, to the result presented in Figure 5, the ceramic foam receiver achieves the highest benefit in terms of the volumetric goodness factor for all the porosities. Also, in both technologies, the optimum porosity is 0.9 where the goodness factor is 2.07×10^5 and 2.29×10^4 for honeycomb mini-channel and ceramic foam receiver, respectively. In both cases, the principal reason for making a decision about the porosity is the amount of power lost in terms of pressure drop, which is minimum for higher porosities despites the possibility of delivering higher temperature outlet when considering lower porosities. Nevertheless, the results in Figure 5 shows that the highest outlet temperature of the fluid is reached for porosities of 0.5 and 0.9 for CF and HC, respectively, and for porosities of 0.9 (the best case in both technologies in terms of the goodness factor), the outlet temperature is higher in the HC than the CF.

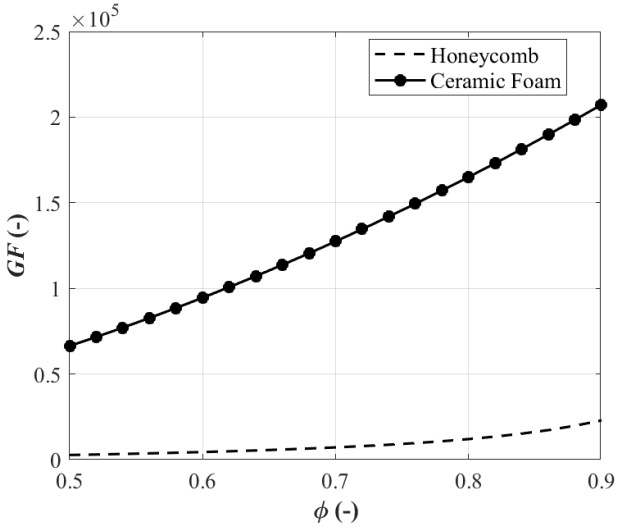

Figure 6. Goodness factor for a honeycomb and ceramic foam receivers, considering different porosities.

4. Conclusions

The present work shows two simplified models, to solve in one dimension the heat exchange process inside two technologies of volumetric receiver and proposes a comparison factor to measure and compare the benefit of both technological proposals, with the objective of maximize the heat transferred to the fluid, incurring in the minimum energy lost by pressure drop. The benefit of that figure of merit considers the energy transferred per unit of time to the working fluid and the power loss due to hydrodynamic resistance of each exchange medium, allowing to

compare two different exchange geometries and consider its principal advantages and disadvantages at the same time. The volumetric goodness factor included in this analysis, explains in a better form the benefit of the devices than other proposed in the literature because it does not consider an average temperature in solid and fluids sides or an approximation as the logarithmic mean temperature difference.

The ceramic foam receiver technology offers more exchange area between both phases (fluid and solid), reducing in 58.3% the necessary length to reach the thermal equilibrium in comparison to honeycomb mini-channel. Furthermore, the amount of solid material is considerably less than the honeycomb proposal.

The honeycomb mini-channel reaches higher fluid outlet temperatures from 629.9 to 679.3 K for porosities over 0.755. The comparison factor is over 9.08 for the complete range of porosity studied in this paper. Reinforcing the idea about the ceramic foam is the best technology, despite the fact of a solid foam porous media has a higher hydrodynamic resistance than a mini-channel exchange media.

Nevertheless, is important to note the contradiction of the optimum selection between both approaches, due to the difference in outlet temperatures at a porosity of 0.9. The volumetric goodness factor shows the design which exchanges energy reducing the hydrodynamic losses, however, higher outlet temperature is also an important factor to take into consideration in the design process. Thus, is necessary to determine a figure of merit able to include the quietly of the outlet energy. This last idea makes reasonable the need for including the entropy concept in a future analysis. The entropy generated considers the effects related to the irreversibilities of the heat transfer process and the hydrodynamic resistance, and additionally include the concept of energy quality, distinguishing the difference between outlet fluids at different temperatures.

5. Acknowledgments

This work was supported by the Chilean Council of Scientific and Technological Research through the Solar Energy Research Center SERC-Chile [CONICYT/FONDAP/15110019].

6. References

Andrienko, D. a., & Surzhikov, S. T. (2012). P1 Approximation Applied to the Radiative Heating of Descent Spacecraft. *Journal of Spacecraft and Rockets*, *49*(6), 1088–1098. https://doi.org/10.2514/1.A32169

Avila-Marin, A. L. (2011). Volumetric receivers in Solar Thermal Power Plants with Central Receiver System technology: A review. *Solar Energy*, *85*(5), 891–910. https://doi.org/10.1016/j.solener.2011.02.002

Bejan, A. (2013). *Convection Heat Transfer*. https://doi.org/10.1002/9781118671627

Bergles, A. E., Junkhan, G. H., & Bunn, R. L. (1976). Performance Criteria for Cooling Systems on Agricultural and Industrial Machines. *SAE Transactions*, *85*, 38–47.

Chen, X., Xia, X. L., Yan, X. W., & Sun, C. (2017). Heat transfer analysis of a volumetric solar receiver with composite porous structure. *Energy Conversion and Management*, *136*, 262–269. https://doi.org/10.1016/j.enconman.2017.01.018

Hsu, C., & Cheng, P. (1990). Thermal despersion in a porous media. *International Journal of Heat and Mass Transfer*, *33*(8), 15871597.

Kaviany, M. (1999). Principles of Heat Transfer in Porous Media. In *Springer*. https://doi.org/10.1007/b22134

Kribus, A., Gray, Y., Grijnevich, M., Mittelman, G., Mey-Cloutier, S., & Caliot, C. (2014). The promise and challenge of solar volumetric absorbers. *Solar Energy*, *110*, 463–481. https://doi.org/10.1016/j.solener.2014.09.035

Kribus, A., Ries, H., & Spirkl, W. (1996). Inherent Limitations of Volumetric Solar Receivers. *Journal of Solar Energy Engineering*, *118*, 151–155.

Krittacom, B., & Kamiuto, K. (2009). Radiation emission characteristics of an open-cellular porous burner. *Journal of Thermal Science and Technology*, *4*(1), 13–24. https://doi.org/10.1299/jtst.4.13

Lage, J., De Lemos, M., & Nield, D. (2012). Mathematical modeling of turbulence in porous media. In *SpringerBriefs in Applied Sciences and Technology*. https://doi.org/10.1007/978-3-642-28276-8_2

Modest, M. (2013). *Radiative Heat Transfer*. Academic Press.

Shah, R. K. (2003). Fundamentals of Heat Exchanger Design. In *Introduction to Thermo-Fluids Systems Design*. https://doi.org/10.1002/9781118403198.ch4

Vafai, K. (2015). Handbook of Porous Media. In CRC (Ed.), *Transport in Porous Media* (Vol. 93). https://doi.org/10.1007/s11242-012-9985-0

Worth, D. J., Spence, A., Crumpton, P. I., & Kolaczkowski, S. T. (1996). Radiative exchange between square parallel channels in a concentric monolith structure. *International Journal of Heat and Mass Transfer*, *39*(7), 1463–1474. https://doi.org/10.1016/0017-9310(95)00222-7

Wu, Z., Caliot, C., Bai, F., Flamant, G., Wang, Z., Zhang, J., & Tian, C. (2010). Experimental and numerical studies of the pressure drop in ceramic foams for volumetric solar receiver applications. *Applied Energy*, *87*(2), 504–513. https://doi.org/10.1016/j.apenergy.2009.08.009

Wu, Z., Caliot, C., Flamant, G., & Wang, Z. (2011a). Coupled radiation and flow modeling in ceramic foam volumetric solar air receivers. *Solar Energy*, *85*(9), 2374–2385. https://doi.org/10.1016/j.solener.2011.06.030

Wu, Z., Caliot, C., Flamant, G., & Wang, Z. (2011b). Numerical simulation of convective heat transfer between air flow and ceramic foams to optimise volumetric solar air receiver performances. *International Journal of Heat and Mass Transfer*, *54*(7–8), 1527–1537. https://doi.org/10.1016/j.ijheatmasstransfer.2010.11.037